Decoherence of Rabi oscillations in laser-generated microplasmas

George Heck, Alex Filin, Dmitri A. Romanov, and Robert J. Levis
Center for Advanced Photonics Research, Department of Chemistry and Department of Physics, Temple University, Philadelphia, Pennsylvania 19122, USA

(Received 31 December 2011; published 22 February 2013; corrected 25 February 2013)

Characteristic fringe patterns of spectral interference in dynamic Rabi sidebands are used as a means to investigate decoherence phenomena in a highly nonequilibrium underdense microplasma formed in atmospheric-pressure oxygen gas in the wake of a strong-field ($\sim 10^{13}$ W/cm^2) femtosecond pump pulse. The same transient processes in the nonequilibrium plasma work both to create the effective two-level systems producing coherent sidebands and to destroy the coherence and smear the sideband spectral structure; the observed spectral fringe pattern is a result of the trade-off of these two effects. The sidebands generated on a moderately intense ($\sim 10^{10}$ W/cm^2) picosecond laser pulse reveal the decoherence rate as a function of the pump-pulse intensity and the pump-probe delay time. The rate increases with the pump laser intensity and decreases with the delay with corresponding decoherence times in the range of 750 fs to 3 ps, in good agreement with theory revealing that electron scattering dominates the dynamics for the subnanosecond relaxation processes.

DOI: 10.1103/PhysRevA.87.023419 PACS number(s): 34.50.Rk, 37.10.Vz, 52.38.Hb, 42.65.Jx

Laser-generated plasmas play a critical role in the propagation of ultrafast, intense laser pulses in gases and gas mixtures at atmospheric pressure since nearly all molecules have appreciable ionization probability at laser intensities above 10^{13} W/cm^2. The dynamics of laser-generated plasmas are important in many related areas of current research, including high harmonic generation [1], attosecond pulse production [2], soft-x-ray lasers [3], and laser filamentation [4]. The free-electron component of a microplasma couples most strongly to the laser field and thus is a major contributor to the propagation in the medium. The electron density and temperature determine also the dynamics of microplasma evolution through electron impact ionization, impact ionization cooling [5,6], and dissociative recombination processes [7].

A number of optical methods have been developed to determine the plasma density dynamics in short-laser-pulse induced plasmas. These include interferometry [8], longitudinal diffractometry [9], Moiré deflectometry [10], folded wave-front interferometry [11,12], and terahertz probe [13]. However, the modification of coherent optical phenomena associated with bound electrons in the constituent atoms, molecules, or ions interacting with the free energetic electrons has not been considered. In particular, the recently discovered dynamic Rabi effect [14,15] emerges in a nonequilibrium plasma and carries information of the plasma characteristics. In the present paper, we advance an approach to monitor the electron dynamics in a laser-generated microplasma on a subpicosecond time scale. This strong-field measurement is based on the spectral manifestations of decoherence processes in dynamic Rabi sidebands.

Quantum coherence is a fundamental hallmark of quantum processes, as it is responsible for regular evolution of a prepared superposition of quantum states. In this capacity, coherence lies at the foundation of a wide variety of diverse phenomena of considerable current interest, for instance, quantum control and quantum computing [16–18]. In particular, quantum coherence is instrumental in the celebrated phenomenon of Rabi oscillation [19–21]. Here, a two-level system driven by a strong electromagnetic field exhibits periodic, out-of-phase oscillations of the ground- and excited-state amplitudes, provided that the coherence is maintained over time intervals longer than the period of such oscillation. The quantum coherence can be lost through two types of decoherence mechanisms: (i) T_1 processes that involve transitions between the two states (or transitions out of the system) that change the magnitude of the state coefficients in the evolving superposition, and (ii) T_2 processes that involve dephasing events that disturb the relative phase between the two coefficients while leaving the magnitudes intact [22]. Evidence for coherence has been measured [14] in the presence of a high-temperature laser-induced microplasma [5,6] where collisional dephasing would be expected to eliminate coherent dynamics. Here, we introduce a pump-probe technique to measure directly decoherence phenomena in a microplasma using spectral fringes in the recently discovered dynamic Rabi sidebands [14]. We have used this technique to investigate the T_2 decoherence in an effective two-state subsystem immersed in a highly nonequilibrium system. We have measured picosecond-range values of the decoherence time and traced their evolution on the subnanosecond time scale after microplasma formation.

The specific system under consideration is atmospheric-pressure oxygen gas that has undergone strong excitation by an ultrashort, intense pump laser pulse ($\sim$60 fs FWHM, $\sim 10^{13}$ W/cm^2 peak focal intensity). This pump pulse leaves in its wake an underdense (10^{19} electrons/cm^3) microplasma that cools and evolves toward equilibrium on a typical subnanosecond time scale [5,6]. In the cooling process, excited oxygen atoms emerge and provide an effective two-state system which is coherently coupled using a moderately intense ($\sim 10^{10}$ W/cm^2) picosecond probe pulse [23,24]. The ensuing induced time-dependent dipole modulates the electromagnetic field at the carrier frequency and generates the radiation forming the Rabi sidebands [14,15,25,26]. Fringes in the sidebands indicate a high degree of coherence in the radiation generated at the leading and trailing edges of the pulse. The loss of coherence reflected in the Rabi sideband emission of excited atomic oxygen is primarily due to collisions with the free electrons in the microplasma during the probe interaction. The method presented here is fundamentally enabled by the

coherence and extent of Rabi sidebands that a highly detuned probe pulse can produce. This method allows for detailed studying of the trade-offs of the two sides of nonequilibrium effects in microplasmas generated in atmospheric-pressure gases by ultraintense, ultrashort laser pulses. Indeed, the highly excited oxygen atoms that supply the broad, coherent, structured sideband signals have themselves emerged in the process of fast plasma evolution. Thus, the same processes in nonequilibrium plasma work to create the effective two-level systems producing coherent sidebands and to destroy the coherence and smear sideband spectral structure. Our observations show how the balance can be shifted by changing the pump-probe delay time and the pump beam attenuation.

The time-dependent oscillation of electronic population in a two-state system with energy levels $\hbar\omega_a$ and $\hbar\omega_b$ occurs at the generalized Rabi frequency, $\Omega'(t) = \sqrt{\Delta^2 + [\mu E(t)]^2}$, when driven by a laser field, where Δ is the detuning between the field carrier frequency (ω_c) and the Bohr frequency ($\omega_{12} = \omega_b - \omega_a$), μ is the dipole transition moment between the two states, and $E(t)$ is the time-dependent envelope amplitude of the linearly polarized electric field of the driving laser pulse. The Rabi oscillation results in time-dependent frequency modulation of the carrier wave producing the dynamic sidebands at frequencies $\omega_c \pm \Omega'(t)$. We have reported observation of large bandwidth (200 meV), structured Rabi sidebands in the emission of excited oxygen atoms present in a microplasma generated by an intense laser pulse, as the plasma evolves toward equilibrium [14,15].

The experimental apparatus has been described in detail previously [14] (see also a cartoon of experimental setup in Refs. [14,15]). Briefly, radiation from a regenerative Ti:sapphire laser (1 kHz, 800 nm, 50 fs, 2.5 W) was split into pump and probe beams. The pump was focused ($\sim 10^{13}$ W/cm^2) using an $f = 10$ cm lens into a chamber of O_2, producing a mix of species including both molecular and atomic ions (O_2^+, O^+), and excited atomic oxygen (O^*). The probe pulse duration was adjusted to 2 ps utilizing a laser line filter and then, at an angle of 90° relative to the pump pulse, was focused into the plasma with an $f = 25$ cm lens. The probe, with a detuning of 46 meV, is coupled to the excited atomic oxygen states: ^5P and $^5S^0$ (transition at 777.3 nm) thus driving Rabi oscillations. The probe beam radius at the focus, 40 μm, is much smaller than the length of the generated plasma formation, ~4 mm, and larger than the width of the plasma formation, 20 μm. Based on these relative sizes, the Rabi sideband emission can be modeled by a quasi-one-dimensional homogeneous distribution of emitting dipoles. Figure 1 shows the blue side Rabi sideband radiation $[\omega_c \pm \Omega(t)]$ detected from the probe pulse interaction with the excited-state oxygen. The characteristic fringes in the power spectrum of the radiated signal can be understood from the mechanism of the dynamic Rabi oscillation. The Rabi frequency, and thus the coherent emission, depends on the amplitude of the driving laser electric field. The picosecond probe pulse has an intensity envelope implying that sideband signals of the same frequency are produced on both the leading and the falling edges of the probe laser pulse. If these same-frequency signals are in (out) of phase, the detected Rabi signal will experience constructive (destructive) interference with a corresponding maximum (minimum) in the spectral fringes. The measured spectrum clearly displays these maxima and minima. In addition to this temporal picture, spatial interference plays a role as well, yielding complicated spatial-spectral interference patterns [14]. As the detected interference fringes are predicated on the time lapse between the modulations of the carrier frequency by the time-dependent dipole produced by the front edge and back edge of the probe pulse they provide a unique instrument for studying decoherence of oxygen atoms when immersed in a heated and chaotic microplasma environment.

A decoherence event that occurs during the course of the pulse will perturb the phase relationship between the radiation emitted at the front and the back of the pulse with accompanying change in the detected signal. In the system under consideration collisions between free electrons and atomic oxygen are the primary source of the decoherence events. A free electron interacting with the atom changes the off-diagonal elements of the Hamiltonian instantaneously changing the values of the energy levels. Such interactions change the Bohr frequency in the effective two-state systems, and, therefore, the detuning, so that the constituent oxygen atoms producing the macroscopic polarization no longer oscillate completely in phase. The evidence for such decoherence in the radiation spectrum is a diminished contrast of the adjacent maxima and minima of the sideband fringes. We define the contrast C as the difference in intensity between a constructive interference maximum value $I_i^{\max}$ and the next (moving from shorter wavelength to longer wavelength) nearest deconstructive interference minimum value $I_i^{\min}$ where $i = 0, \ldots, 5$ (see Fig. 1). In Fig. 1, the sideband interference fringes are presented for two different delays between the plasma-generating pump and the dipole-radiation-driving probe pulses. The fringe pattern in the spectrum of the 753-ps delay experiment clearly shows

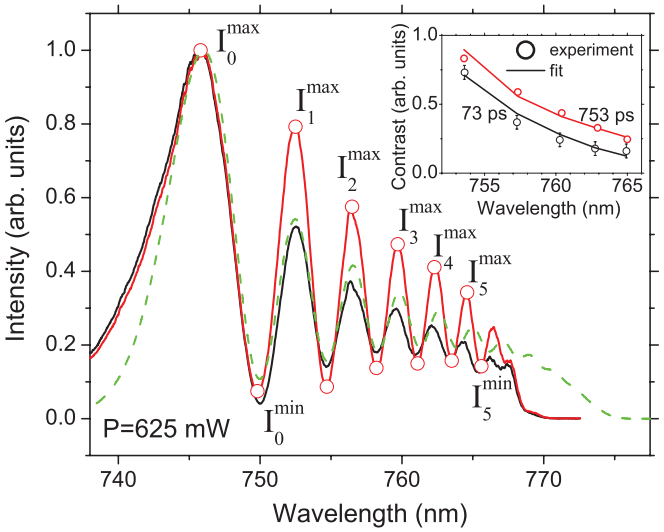

FIG. 1. (Color online) Typical Rabi spectra used for dephasing analysis. Black and red solid curves represent the spectra measured under pump power $P = 625$ mW at the delays 73 and 753 ps, respectively. Dashed curve is the fitting for the 73 ps spectrum. Hollow circles give the positions of maxima and minima of fringes. Inset shows the wavelength dependence of fringes' contrast derived from the presented curves as described in the text.

greater contrast values in comparison to the 73-ps delay experiment. This trend is expected, because the number of electron-atom collisions decreases while the plasma evolves toward equilibrium, as we discuss later in more detail.

In order to determine the values of dephasing time as a function of pump-probe delay, fitting was done comparing the experimental contrast and those found using computer simulations incorporating a dephasing time parameter. Specifically, solving the density-matrix equations in the relaxation time approximation, we find the time dependence of the induced dipole oscillations,

$$\mu(t) = \exp(-\gamma t)\sin\theta\Big(\exp[-\gamma t + 2\gamma\tau(t)] \times \exp[-\gamma\tau(t)]\Big\{\cos^2\left(\frac{\theta}{2}\right)\cos[\omega t - \varphi(t)] - \sin^2\left(\frac{\theta}{2}\right)\cos[\omega t + \varphi(t)]\Big\}\Big), \quad (1)$$

where

$$\theta(t) = \tan^{-1}\left[\frac{\mu E(t)}{\Delta}\right]; \quad \varphi(t) = \int dt\Omega'(t); \quad \tau(t) = \int dt\frac{\Delta^2}{[\Omega'(t)]^2}, \quad (2)$$

and γ is the dephasing rate (the inverse dephasing time). The two terms in the second line of Eq. (1) give rise to the red-shifted and blue-shifted Rabi sidebands, respectively, in the dipole-emitted radiation. As this oscillating dipole is driven by the laser field, $E(t)$, each available value of instantaneous frequency in these sidebands occurs twice: at the leading edge of the laser pulse and at the trailing edge. This results in spectral interference and, given the spatial distribution of the driven two-level systems, produces characteristic spatial-spectral distribution patterns detected at a distance [14,25,26].

The numerical fitting procedure used to analyze the data is constructed using a previous model for the Rabi sideband spectra for atomic oxygen in nonequilibrium microplasma for a number of different driving laser pulse shapes [25,26]. The fitting was done by comparing experimental and simulated contrast values because the contrast is directly related to the dephasing processes and is not affected by other parameters of the system, such as plasma homogeneity, and therefore the contrast values contain all the relevant information necessary for the determination of the dephasing time. Two main criteria were used in the fitting process: (i) best coincidence of experimental and theoretical minima or maxima spectral positions and (ii) minimization of mean square deviation of contrast C. To determine coherence lifetimes over a range of electron densities and velocities, the emitted Rabi radiation from the two-state oxygen system was recorded at four values of the pump-probe delay (73, 274, 540, and 742 ps) and for three values of the pump-pulse powers (525, 575, and 625 mW). (The focal-volume intensities corresponding to these values of the pump power are 1×10^{10}, 3×10^{10}, and 4×10^{10} W/cm^2.) The contrast C versus wavelength as a function of the delay between pump and probe pulses at the pump energy of 575 mW is shown in Fig. 2. The clear trend of increasing contrast with longer delay follows from the model of decreasing collision rates, as the plasma cools.

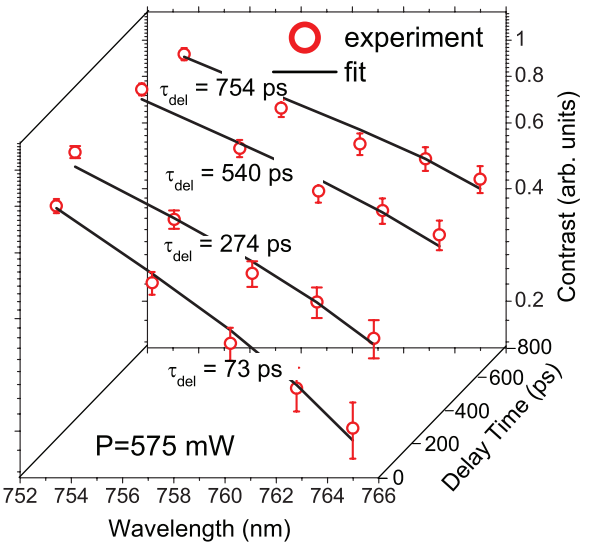

FIG. 2. (Color online) Wavelength dependence of the contrast as a function of the pump-probe delay.

The results for the dynamic dephasing times which give the closest fit of simulated contrast curves to the experimental contrast curves are shown in Fig. 3. The linear dependence of the decoherence time on the pump-probe delay can be captured in the following simple model of the plasma dynamics. The main source of decoherence of the two-level system is collisions with free electrons that are much more mobile than slow molecules, atoms, or ions. A passing electron disturbs the relative phase of the two-state system by the action of its electric field, $E_{el}(t) = e/r^2(t)$. The resulting phase shift by a single collision act is obtained in a form similar to the Bloch-Siegert shift:

$$\Delta\varphi = 2\frac{\mu^2 e^2}{\hbar^2\omega_{12}}\int_{-\infty}^{\infty} dt(a^2 + v^2t^2)^{-2} = \frac{\pi\mu^2 e^2}{\hbar^2\omega_{12}a^3 v}. \quad (3)$$

Here, v is the velocity of the colliding electron and a is the impact parameter. Averaging the corresponding change in the density matrix over the values of a and the electron velocity distribution results in the following expression for the

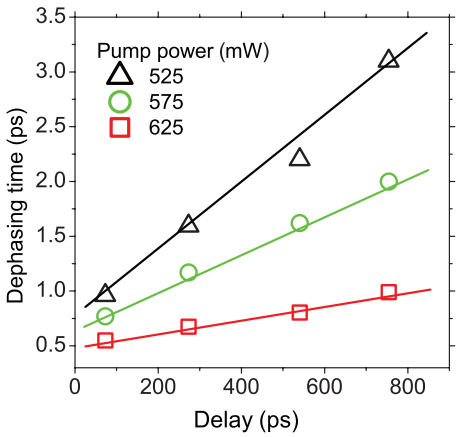

FIG. 3. (Color online) Dephasing time versus delay for three various values of the pump-pulse power. (Symbols) experiment, (straight lines) linear fit.

dephasing rate:

$$\gamma = 8N\left(\frac{\pi}{3}\right)^{3/2}\left(\frac{kT}{2m}\right)^{1/6}\left(\frac{\pi\mu^2e^2}{\hbar^2\omega_{12}}\right)^{2/3}. \quad (4)$$

In this expression, N and T are the electron gas density and temperature. Note that the dependence of dephasing on the electron temperature is effectively minimized, as compared with the case of atom-atom collisions, due to the following two competing effects. While the increase in electron temperature leads to a greater frequency of collisions, the higher temperature also decreases the duration of each collision, correspondingly decreasing the phase shift incurred.

The dependence of the electron density and temperature on the time delay after the initial excitation is determined by complicated processes of the electron gas cooling and attrition due to interaction with neutral and ionized atoms or molecules. In particular, earlier investigations of electron dynamics in O_2 based cold plasma have demonstrated that in the case of relatively low initial electron concentrations [$n_e(0) < 6 \times 10^{17}$ cm^{-3}] and temperatures, the dependence of T_e on time is insignificant [13]. This makes for a hyperbolic dependence of electron density $n_e(t)$ as follows. The main mechanism for electron density evolution is the dissociative recombination of free electrons with the molecular oxygen molecular ions: $O_2^+ + e^- = O + O^*$. This attrition process is described by the simple rate equation,

$$\dot{n}_e = -\beta(T_e)n_e n_{O_2^+} = -\beta(T_e)n_e^2. \quad (5)$$

Here, $\beta(T_e)$ is the electron-temperature-dependent attrition rate coefficient, and $n_e = n_{O_2^+}$ is assumed at all times as there are no other cations in the system. If $T_e = \text{const}$, Eq. (5) is easily solved [13] to produce

$$\frac{1}{n_e(t)} = \frac{1}{n_e(0)} + \beta(T_e)t. \quad (6)$$

According to Eq. (4), the dephasing time $\tau_{\text{deph}} = 1/\gamma$ is inversely proportional to n_e and thus one should expect linear dependence of τ_{deph} on the delay time between the initial excitation of the system and the arrival of a Rabi-sideband-inducing picosecond laser pulse.

In conclusion, we have demonstrated that the spectral fringe patterns of broad, structured Rabi sidebands can be used to study relatively short (in picosecond range) decoherence times for a coherently evolving two-state system driven by an intense ($\sim 10^{10}$ W/cm^2) picosecond laser pulse. The two-state system was generated in highly nonequilibrium oxygen microplasma generated by an intense, $\sim 10^{13}$ W/cm^2, femtosecond duration laser pulse. We have established the decoherence rate as a function of the intensity of the plasma-generating laser pulse, and we have traced the evolution of the decoherence rate as the microplasma evolved toward equilibrium. The measured power and time dependence of the decoherence process are in good agreement with theoretical models. The measurements reveal that the decoherence dynamics proceed on a subpicosecond to a few picosecond time scale for an effective two-state system in a laser-generated microplasma.

We acknowledge the support of the National Science Foundation Grant No. CHE0957694.

[1] A. L'Huillier and P. Balcou, Phys. Rev. Lett. **70**, 774 (1993).
[2] N. A. Papadogiannis, B. Witzel, C. Kalpouzos, and D. Charalambidis, Phys. Rev. Lett. **83**, 4289 (1999).
[3] H. M. Milchberg, C. G. Durfee III, and J. Lynch, J. Opt. Soc. Am. B **12**, 731 (1995).
[4] J. Kasparian, M. Rodriguez, G. Méjean, J. Yu, E. Salmon, H. Wille, R. Bourayou, S. Frey, Y. B. Andre, A. Mysyrowicz, R. Sauerbrey, J. P. Wolf, and L. Woeste, Science **301**, 61 (2003).
[5] A. Filin, R. Compton, D. A. Romanov, and R. J. Levis, Phys. Rev. Lett. **102** 155004 (2009).
[6] D. A. Romanov, R. Compton, A. Filin, and R. J. Levis, Phys. Rev. A **81**, 033403 (2010).
[7] A. Petrignani, W. J. van der Zande, P. C. Cosby, F. Hellberg, R. D. Thomas, and M. Larsson, J. Chem. Phys. **122**, 014302 (2005).
[8] H. Yang, J. Zhang, Y. Li, J. Zhang, Y. Li, Z. Chen, H. Teng, Z. Wei, and Z. Sheng, Phys. Rev. E **66**, 016406 (2002).
[9] J. Liu, Z. Duan, Z. Zeng, X. Xie, Y. Deng, R. Li, Z. Xu, and S. L. Chin, Phys. Rev. E **72**, 026412 (2005).
[10] M. Dunne, T. Afshar-Rad, J. Edwards, A. J. MacKinnon, S. M. Viana, O. Willi, and G. Pert, Phys. Rev. Lett. **72**, 1024 (1994).
[11] T. R. Clark and H. M. Milchberg, Phys. Rev. Lett. **78**, 2373 (1997).
[12] Y. H. Chen, S. Varma, T. M. Antonsen, and H. M. Milchberg, Phys. Rev. Lett. **105**, 215005 (2010).
[13] T. Kampfrath, D. O. Gericke, L. Perfetti, P. Tegeder, M. Wolf, and C. Frischkorn, Phys. Rev. E **76**, 066401 (2007).
[14] R. Compton, A. Filin, D. A. Romanov, and R. J. Levis, Phys. Rev. Lett. **103**, 205001 (2009).
[15] R. Compton, A. Filin, D. A. Romanov, and R. J. Levis, Phys. Rev. A **83**, 053423 (2011).
[16] R. Hildner, D. Brinks, and N. van Hulst, Nat. Phys. **7**, 172 (2011).
[17] D. Press, T. Ladd, B. Zhang, and Y. Tamamoto, Nature **456**, 218 (2008).
[18] H. Specht C. Nölleke, A. Reiserer, M. Uphoff, E. Figueroa, S. Ritter, and G. Rempe, Nature **473**, 190 (2011).
[19] I. I. Rabi, Phys. Rev. **51**, 652 (1937).
[20] Y. Yu, S. Han, X. Chu, S. I. Chu, and Z. Wang, Science **296**, 889 (2002).
[21] I. Chiorescu, Y. Nakamura, C. J. P. M. Harmans, and J. E. Mooij, Science **299**, 1869 (2003).
[22] L. Allen, J. Eberly, *Optical Resonance and Two Level Atoms* (Wiley, NewYork, 1975).
[23] G. Rodriguez, A. R. Valenzuela, B. Yellampalle, M. J. Schmitt, and K.-Y. Kim, J. Opt. Soc. Am. B **25**, 1988 (2008).
[24] Z. Wu, H. Cai, H. M. Milchberg, and H. Zeng, Phys. Rev. A **82**, 043431 (2010).
[25] M. Plewicki, R. Compton, A. Filin, D. A. Romanov, and R. J. Levis, Opt. Lett. **35**, 778 (2010).
[26] G. Heck, R. Compton, A. Filin, M. Plewicki, D. A. Romanov, and R. J. Levis, Opt. Lett. **36**, 3224 (2011).